UNIVERSITY OF CALIFORNIA — BERKELEY

RADIATION LABORATORY

DISCLAIMER

UCRL-1967
Unclassified-Physics Distribution

UNIVERSITY OF CALIFORNIA

Radiation Laboratory

Contract No. W-7405-eng-48

NUCLEAR ABSORPTION CROSS SECTIONS FOR HIGH ENERGY PROTONS

Albert John Kirschbaum
(Thesis)

October, 1952

Berkeley, California

TABLE OF CONTENTS

NUCLEAR ABSORPTION CROSS SECTIONS FOR HIGH ENERGY PROTONS

Albert John Kirschbaum

INTRODUCTION

The fundamental problems of nuclear physics are the study of the structure of the nucleus, the behavior of nucleons within the nucleus, and the nucleon-nucleon forces that are responsible for this structure and behavior. The most direct information about nucleon-nucleon forces is obtained from the investigation of the n-p and p-p scattering cross sections as functions of energy and angle of scatter. Information about the properties of nuclear matter and the behavior of nucleons within a nucleus is obtained from detailed measurement of the elastic, inelastic, and total cross sections of representative nuclei under bombardment by high energy nucleons. Most of the research of this type has been performed using neutron beams.[1-8]

The results of these experiments can be summarized very briefly as follows: At low energies--15 Mev to 45 Mev--the total nuclear cross sections are quite constant with respect to energy and follow an $A^{2/3}$ law. From this one concludes that in this energy range the mean free path of the incident particle in nuclear matter is small compared to the nuclear dimensions and hence the nucleus is an opaque sphere. The $A^{2/3}$ law implies constant nucleon density and from the measured cross sections one finds the best fit with $R = A^{1/3} \times 1.37 \times 10^{-13}$ cm. It was found that $\sigma(\text{elastic}) = \sigma(\text{inelastic}) = 1/2\ \sigma(\text{total}) = \pi R^2$ which supports the opaque sphere hypotehsis. As the energy of the bombarding nucleon was raised above 45 Mev for light elements such as C, Be, Al,

and above 80 Mev for heavy elements such as Pb and U, the total cross sections were found to decrease quite rapidly. One must either assume that the effective nuclear radius shrinks with increasing bombarding energy, i.e., that much of the previously defined nuclear radius includes a nuclear force field that extends a considerable distance beyond the nuclear surface; or, one must assume that the nucleus becomes partially transparent to the incident nucleon. Both phenomena probably take place, but because of the extremely short range nature of nuclear forces the bulk of the variation in the cross section, over the energy range 45 to 280 Mev, is attributed to the transparency effect. Fernbach, Serber, and Taylor[9] have formulated a theory of the transparent nucleus to explain this phenomenon quantitatively. Reasonable agreement exists between the experimental values of σ(total) and the predicted values for energies up to approximately 200 Mev. Above 200 Mev the measured cross sections appear to flatten out and the agreement is poor, since the theory predicts a decrease in σ(total) which depends upon the fall off in the n-p and p-p cross sections with energy. A more stringent test of the details of the theory can be obtained by measuring the σ(elastic) or diffraction cross section, and the σ(inelastic) or absorption cross section.

According to the transparent nucleus theory, the nucleus is treated as a partially transparent sphere characterized by an absorption coefficient and a refractive index. The values to be used for the absorption coefficient and refractive index are determined by the results of other independent measurements. Thus, the absorption coefficient depends upon the free nucleon-nucleon cross sections and the nucleon

density within the nucleus. The refractive index depends upon the mean potential energy V of the incident nucleon when inside the nucleus.

For neutrons incident:

1) Abs. coeff. = $K = \frac{3A\bar{\sigma}}{4\pi R^3}$, where $\bar{\sigma} = \frac{Z\sigma_{np} + (A - Z)\sigma_{nn}}{A}$

σ_{np} and σ_{nn} = nucleon-nucleon cross sections at the appropriate energy, modified by the exclusion principle which prohibits low energy transfer collisions.

R = nuclear radius = $1.37\ A^{1/3} \times 10^{-13}$ cm.

A = atomic mass.

2) Propagation vector inside the nucleus = $k + k_1 = k\left[1 + V/E\right]^{1/2}$

k = propagation vector outside the nucleus

$k + k_1$ = propagation vector inside nucleus

V = mean nuclear potential

E = bombarding energy

The total cross section and the elastic or diffraction cross section are functions of both k and k_1. The effective index of refraction enters in an extremely complex manner, and the measurement of σ(total) or σ(elastic) yields results difficult to analyse. On the other hand, σ(inelastic) or the absorption cross section, as Serber calls it and as we shall refer to it hereafter, is a simple function of k, the absorption coefficient, and R, the nuclear radius.

$$\frac{\sigma_a}{\pi R^2} = 1 - \frac{1 - (1 + 2KR)\, e^{-2KR}}{2K^2R^2}$$

(See Fig. 7 for a plot of this function.)

The measurement of σ (absorption) thus gives direct information about the quantity K, which in turn is related to the individual cross sections for the incident high energy nucleon and the nucleons within

the nucleus. Thus, in principle, here is an experiment where one can compare the σ (p-p) and σ (n-n), since in the formula for K, $K = \frac{3 A \bar{\sigma}}{4\pi R^3}$ with $\bar{\sigma} = \frac{Z \sigma_{np} + (A - Z) \sigma_{nn}}{A}$ for neutrons incident, and $\bar{\sigma} = \frac{Z \sigma_{pp} + (A - Z) \sigma_{np}}{A}$ for protons incident. The necessary accuracy for such a comparison has not yet been obtained, due to inherent difficulties in both neutron and proton absorption cross section experiments. We see though that measurement of σ(absorption) for protons yields a check on the theory since σ (n-p) and σ(p-p) are known, for free nucleon collisions.

Using neutron beams one can quite readily measure σ (total) by a good geometry experiment using a few mean free paths of attenuator. The measurement of σ(diffraction) or σ(absorption) is difficult, however, since high energy neutron beams are far from monochromatic and good energy sensitive direct neutron detectors do not exist for energies above 60 Mev. It is therefore difficult to separate the elastically scattered neutrons from those inelastically scattered.

Measurements have been made[7] which in effect place a lower limit on σ(absorption) and an upper limit on σ(diffraction). Recently, W. Ball,[8] measured σ (absorption) and σ(diffraction) for neutrons using a recoil proton counter as the energy sensitive neutron detector. The results of this experiment are given in Table II.

The use of protons to investigate the nucleus has two distinct advantages. The high energy proton beam is monochromatic to a few percent at least, and by the use of absorbers, energy sensitive counters can be employed. A great disadvantage exists, however, in that, because of ionization loss in the attenuator, only a small fraction (approximately

1/10) of a mean free path can be used if one is to measure the cross section over a reasonably narrow energy band. Thus, the quantity in which we are interested must be measured by the small difference of two large numbers. This reduces the accuracy of any measurement of σ by beam attenuation. (In the discussion of errors in the results it will be shown that although the ratio of the number of protons entering and leaving the absorber is known to 0.5 percent, the cross section is known only to 10 percent.)

In addition to whatever theoretical value might be ascribed to the proton absorption cross sections, the measured attenuation factors are of practical interest to experimenters who must correct their data for this effect because of the use of absorbers.

On the basis of the above considerations it was decided to attempt measurement of the absorption cross sections of a representative group of elements for protons in the energy range 160-340 Mev and with as many separate energy bands as seemed reasonable. We will now consider briefly the method employed to measure σ (absorption) for high energy protons on the six elements Be, C, Al, Cu, Pb, and U, and also the difficulties that must be anticipated using such a method.

Basically what we must do to measure σ (absorption) is to count the number, N_o, of protons entering the attenuator and the number, N_1, leaving it with an energy equal to the incident energy minus the energy lost by ionization in the attenuator. The difference of these two numbers is then the number lost by inelastic collisions with the nuclei. Expressed mathematically, $N_1 = N_o e^{-n\sigma_a}$

where n = nuclei per cm^2 in attenuator

N_o = no. of protons entering attenuator

N_1 = no. of protons leaving attenuator

σ_a = absorption cross section

Multiple coulomb scattering and diffraction scattering do not appreciably degrade the energy of the protons. In the worst case to be considered in this experiment, that of a 20° diffraction scatter from Be^9, the proton loses 5 Mev to the recoiling Be nucleus. The effect of diffraction scattering and multiple coulomb scattering must be considered in determining how "poor" the geometry of the experiment must be.

Figures 1 and 2 indicate the manner in which the equipment is arranged. The cyclotron is operated at an extremely low level, so that approximately 30 protons per second enter the equipment. Counters 1 and 2 in coincidence count the individual protons as they enter any of the various attenuators. Counter 3 in coincidence with 1 and 2 counts only those protons which leave the attenuator with no additional loss in energy than that due to ionization. This is achieved by placing sufficient copper in front of counter 3 to stop all protons that lose in the attenuator 20 Mev or more, in addition to ionization loss. Counter 3 is thus properly energy sensitive, but it now has an unknown efficiency since many protons will be lost by inelastic collisions in the copper absorber. If attenuators that are equivalent in stopping power are used, their relative cross sections can be calculated from the data so far obtained, since the efficiency of counter 3 is the same for each of the attenuators. To determine an absolute cross section the efficiency of counter 3 with the copper absorber in front of it must be measured.

This is done by placing at the exit end of the magnetic channel a piece of copper, equivalent in stopping power to the attenuators. (See Fig. 1.) Then by retuning the focus magnet a monoenergetic beam of protons of the same energy as those that left the attenuator with no inelastic collisions can be passed through the counting system. The different angular spread in the beam, with and without the attenuator, is compensated for, by using a shaped rear absorber, so that all protons have the same path length in the absorber. The ratio of counter 1, 2, 3 coincidences to counter 1 and 2 coincidences gives the efficiency of energy sensitive counter 3. Using this efficiency we now have

$N_2 = \varepsilon N_1 \quad \therefore \quad N_2 = \varepsilon N_o \, e^{-n\sigma}$, with

N_o = no. of protons entering attenuator

N_1 = no. of protons leaving attenuator (not measured directly)

N_2 = no. of protons leaving attenuator and copper abs.

ε = efficiency of counter no. 3 as determined by the calibration run with internal absorber

n = no. of nuclei/cm^2 in attenuator

σ_a = absorption cross section for attenuator nuclei.

DESCRIPTION AND REQUIREMENTS OF EXPERIMENTAL APPARATUS

Counter No. 1

Counter No. 1 must detect a 1/2 in. diameter beam of protons over the energy range 340-160 Mev, with efficiency reasonably close to 100 percent. It consists of a 2.5 cm x 2.5 cm x 1 cm clear stillbene crystal mounted on a 1P21 phototube. The phototube chassis is wired in the conventional manner. The negative signal from the anode is fed over double shielded 125 ohm line to the linear amplifier in the counting area. The cable is properly terminated to avoid ringing.

Counter No. 2

Counter No. 2 must detect protons in the beam the same as counter No. 1, and in addition must discriminate against two protons that occur within the resolving time (0.5 μ sec.) of the coincidence circuit used. This is necessary since two protons less than 0.5 μ sec. apart will be counted as a single proton entering the attenuator, but the total probability of a count in counter No. 3 due to either of them is just twice what it is for a single proton entering the system. Thus double protons would reduce the measured cross sections. (With a 15 microsecond beam pulse, 50 times per second, the probability of two protons less than 0.5 μ sec. apart with a beam of 30 protons per second is $\frac{0.5 \times 30}{15 \times 50} \approx$ 2 percent.) Because pulse height is to be used to discriminate against two protons, Counter No. 2 consists of a 5 cm x 2.5 cm x 0.6 cm perfect stillbene crystal mounted between two 1P21 phototubes. The output signals from the anodes are combined by short lengths of shielded cable of known capacity, and are fed into a 6AH6 cathode follower. The input

impedance of the cathode follower and capacity of the cable and 1P21 anodes form an RC circuit with a time constant of 1 μ sec. The pulses from two protons less than 1/2 μ sec. apart will be added by the RC circuit, and, depending upon their separation in time, will give an output pulse between 50 percent and 100 percent higher than a single proton pulse. This higher level pulse can be used to activate an anti-coincidence channel and thus reject those signals from multiple protons. Protons further apart in time than 1/2 μ sec. are separated by the coincidence circuit used. The signal from the cathode follower is in turn fed through double shielded cable to a linear amplifier in the counting area.

It should be remarked here that the pulse height properties of such a system, with an RC circuit to integrate the current passed by the phototubes, are much superior to one where the output pulse height is determined by the peak current passed by the tubes. This is particularly true when two or more tubes are used in parallel to view the same scintillator.

The pulse height spread of the system can be estimated roughly by the following simple considerations: If

$N \cong$ no. of photo electrons

$\Delta E \cong 2$ Mev $\cong$ energy loss in crystal

$\mathcal{E} \cong 200$ ev $\cong$ average ionization loss per photon emitted

$\Omega \cong 0.1 \cong$ light collection efficiency

$\gamma \cong 0.05 \cong$ photocathode efficiency

Then

$$N \cong \frac{\Delta E}{\mathcal{E}} \times \Omega \times \gamma \cong 50$$

$$\therefore \frac{\delta N}{N} \cong \frac{\sqrt{50}}{50} \approx 15 \text{ percent.}$$

Thus the full width at half maximum of the pulse height distribution for 340 Mev protons should be of the order of 30 percent. This is sufficient resolution to distinguish between one and two protons as discussed above. The experimental check of this number will be described in the section on experimental procedure.

Counter No. 3

Because of diffraction scattering and multiple coulomb scattering, counter No. 3 must be of large enough area to provide the necessary poor geometry. The areas presented to the beam by the attenuators, copper absorbers, and counter No. 3 are so chosen that all protons scattered in a cone of half angle 22.5° are contained. (See Fig. 3). The scintillator for counter No. 3 consists of a solution of three grams of terphenyl per kilogram of phenylcyclohexane, with 15 miligrams of diphenylhexatriene per kilogram of solution added to concentrate the radiated light about a wave length of 5000 A, the region of maximum sensitivity of the 5819 photocathode. The liquid is held in a lucite container 9 in. in diameter and 2 in. thick. The lucite walls of the cylinder are 1/2 in. thick, and the lucite faces are 1/8 in. thick. It is viewed from the back by a magnetically shielded 5819, 6 in. from the scintillator. (See Fig. 2). A silvered mirror mounted on the front face of the counter is the only aid to light collection used, since a tapered lucite light pipe or conical reflector would not improve the light collection appreciably. Also, since the protons lose at least 50 Mev in this counter, there is no problem in the detection of these particles. The counter is tested with 340 Mev protons which lose 15 Mev in the scintillator. In such tests, it counts with 100 percent efficiency.

The signal from the 5819 is fed to an RC circuit and cathode follower similar to that used for counter No. 2. This increases the signal to noise ratio, since the noise pulse peak currents from the 5819 are comparable to the signal peak currents, but the integrated current or charge from a noise pulse is not as great as that from a signal, in general.

Attenuators and Absorbers

The thickness of the attenuators is calculated using the range energy curves to obtain the grams per cm^2 of copper required for the desired stopping power, and then using the relative stopping powers as measured by Bakker and Segrè[10] to calculate the grams per cm^2 for the other five elements used. The C, Al, Cu, and Pb attenuators are accurately machined blocks of the proper thickness, as calculated from the published densities. The densities are checked by weighing the attenuators and determining their volume by vernier caliper measurements.

Because of the difficulty in obtaining Be and U, these absorbers are built up of several borrowed pieces with unmachined edges. Their thickness for the proper grams per cm^2 is calculated from the density values as measured previously by the group from whom they were borrowed. The possible error in the densities (less than 1 percent) is small compared to other errors in the experiment.

The copper absorbers are selected flat stock or are machined to the desired thickness. Using various combinations any thickness up to 4 in., in 1/64 in. steps, can be obtained. For the 335-270 Mev and the 270-205 Mev energy bands, a shaped rear absorber is used. (See

Fig. 3). With such a shaped absorber the knee of the range curve (See Fig. 8) is sharper. The shaped absorber compensates for the additional path which protons, that have been multiple coulomb scattered or diffraction scattered through a large angle, would normally have to traverse. The internal absorbers for reducing the energy of the proton beam are 6 in. square copper plates of exactly the same thickness as the copper attenuators used.

Electronic Equipment

The linear amplifiers, variable gate units, and ten channel quadruple coincidence circuit used are all standard UCRL equipment, available in the counting area racks. The pertinent characteristics of each are:

Linear amplifier

1. Gain continuously variable from 250-8000
2. Band pass of 8 megacycles
3. Input time constant 5 microseconds.

Variable gate units

1. Calibrated discriminator 0.0-100 volts
2. Variable delay of 0.5 μsec. to 10 μsec.
3. Variable output pulse width of 0.5 to 10 μsec.
4. Dead time of 3 μsec.

Ten channel coincidence mixer

1. Ten inputs and ten quadruple coincidence outputs
2. Anti-coincidence available on 4th input of each of the ten mixer channels.
3. Resolving time of twice the pulse width used, for pulses at least 0.1 μsec. wide.

EXPERIMENTAL PROCEDURE

Collimation, Alignment, and Beam Reduction

Using the maximum intensity 340 Mev scatter deflected proton beam with the pre-magnet collimator wide open, the focus magnet is adjusted and the 1/2 in. by 48 in. collimator is carefully aligned with respect to the beam for minimum spray from the walls of the collimator. When the pre-magnet collimator is then closed down to 0.07 in. high by 0.12 in. wide, the beam passes cleanly down the 1/2 in. collimator without touching the walls. When the internal absorbers are placed in the beam, it is felt that if the focus magnet is retuned for maximum beam in the cave, as determined by counters No. 1 and No. 2, that the beam will have a minimum amount of low energy spray. This assumption is checked later on by taking a range curve at all beam energies. With internal absorbers, pictures of the beam are not possible because of the greatly reduced beam intensity.

Still using the full intensity beam, the equipment is easily aligned by positioning screws so that the center line of the three counters coincides with the beam center line within 1/8 in.

The beam is now reduced to 30 protons per second in the following manner. The arc pulse and gas flow are turned off, and the filament current is reduced about 10 percent. A beam clipper located at approximately a 20 in. radius is lowered into the internal proton beam until the desired counting rate is achieved. By varying the filament current it is possible to control this beam, and to hold the beam level constant to 20 percent without undue effort. When internal absorbers are used, the circulating beam must be raised by factors on the order

of a million. This is because of the small solid angle the pre-magnet collimator opening subtends, and the multiple coulomb scattering in the internal absorber which is approximately ten feet away. With the maximum amount of internal absorber used, 2.91 in., the cyclotron must be run at full intensity to obtain 30 protons per second in the cave.

Plateaus in Counters No. 1 and No. 3

To determine the proper operating voltages for counters No. 1 and No. 3 a counts versus high voltage curve is taken for each counter in the following manner. Using counters No. 2 and No. 3 in coincidence as a monitor, the number of coincidences between counters 1 and 2 are plotted as a function of the high voltage on counter 1. With the counter 1 linear amplifier set at 250 and the variable gate discriminator set at 15 volts, the plateau extends from 1100 volts to 1300 volts. 1200 volts is the operating point chosen for this 1P21.

In a similar manner using counters 1 and 2 in coincidence and counters 1 and 3 in coincidence a plateau is found for counter 3. In this case, the counter 3 linear amplifier gain is set at 8000, and the plateau extends from 800 to 950 volts. The 5819 is operated at 875 volts. Operating with a lower amplifier gain and higher voltage decreases the signal to noise ratio of this tube.

Adjustment of Pulse Height Counter No. 2

We must first adjust the high voltages on the two tubes viewing counter 2 so that on the average they give output pulses of equal height. With the discriminator set at 15 volts, the linear amplifier gain set at 2000, and high voltage applied to each of the tubes separately, the

counting efficiency of each tube is adjusted, by varying its high voltage, to one-half its plateau value. That is, until coincidences 1 and 2 are half coincidences 1 and 3. This is the point of steepest slope on the initial rise of the counting efficiency versus high voltage curve, and thus allows one to adjust the tubes to equivalent operation with the greatest accuracy.

With the high voltages on the tubes set for equal sensitivity the linear amplifier gain is then adjusted until the coincidence channel for this counter accepts all proton pulses. (See Fig. 6). The anti-coincidence channel is then activated and the discriminator for this channel adjusted to the point shown on Fig. 6. This is the point at which counters 1 and 2 in coincidence, with the anti-coincidence circuit operating, count approximately one-half as many protons as counters 1 and 2 in coincidence only. This is a rather drastic condition to impose upon the pulse height of the signals from counter 2, but it insures the exclusion of double protons. The pulse height resolution of counter 2 is studied by taking a differential discriminator curve at a low enough beam to insure only single protons. At 10 protons per second the chance of two protons less than 1/2 μ sec. apart is 0.7 percent. The full width at half maximum of this curve is 40 percent, as compared to 30 percent predicted theoretically.

Range Curve

With the counters adjusted as described above, an integral range curve is taken using the copper attenuator and copper absorbers. (See Fig. 8). The purpose of this curve is fourfold:

1) To check the beam energy (most important at the lower energies)

2) To check for low energy contamination

3) To locate a running point above the knee of the curve

4) To locate a check point (the point of steepest slope) at which to compare the stopping power of the various attenuators.

With the copper attenuator replaced by the various attenuators, the location of the running point and range point is checked in terms of the amount of copper absorber required.

Cross Section Runs

The actual cross section data is now taken in three separate runs on each attenuator and the consistency of the ratios of triple to double coincidences is taken as a measure of the stability of the equipment. Several additional checks are made during these runs. The ratio of triple coincidences to double coincidences is checked under the following conditions:

1) When the counting rate is doubled or halved by changing the beam level, the ratios remain constant to 1/2 percent

2) Counter 3 is moved back in 1 in. steps to check the poor geometry. No change in the ratio is detected for a change in position of 3 in. or less. At 5 in. the ratio decreases by 3 percent

3) The effective discrimination against double protons is varied by increasing the linear amplifier gain for counter 2 by 10 percent. This changes the fraction of counter 2 pulses accepted by the electronics from 50 percent to 16 percent. No change in the triple coincidence to double coincidence ratio is detected.

4) With no attenuators or external absorbers the ratio of triples to doubles is checked to determine any sag in the detection efficiency of counter 3. Its efficiency did not change by more than 0.1 percent.

Reduction of Beam Energy

The internal absorber is now run in on the proton cart, and positioned so that all the beam from the magnetic channel has to pass through this absorber. The internal beam of the cyclotron is raised the required amount, and the focus magnet is then retuned for maximum beam in the cave. A range curve is then taken and compared to the full energy, "clean" beam range curve to check the beam energy, and to detect any low energy spray. (See Fig. 8).

Calibration of Counter No. 3 Efficiency

With exactly the same copper absorbers that were used in the previous cross section runs, the efficiency of the energy sensitive counter 3 is now measured by comparing counter 1, 2, and 3 coincidences against counter 1 and 2 coincidences.

Cross Section Measurements for Lower Energy Bands

With the appropriate internal absorber to reduce the beam energy the steps outlined above are repeated to measure the cross sections for the two lower energy bands.

CALCULATIONS

Cross Section Calculations

With the attenuator let:

N_o = no. of protons entering the attenuator

N_2 = no. of protons leaving the absorber.

With no attenuator, but with a corresponding internal absorber let:

N_o' = no. of protons entering the absorber

N_2' = no. of protons leaving the absorber.

Let ε = efficiency of counter 3 with copper absorber in front of it

σ_a = absorption cross section of attenuator nuclei

n = no. of atoms/ cm^2 in attenuator.

Then $\varepsilon = \frac{N_2'}{N_o'}$

and $N_2 = \varepsilon N_o e^{-n\sigma} = \frac{N_2' N_o}{N_o'} e^{-n\sigma}$

$\therefore \sigma = \frac{1}{n} \ln \frac{N_2' N_o}{N_o' N_2}$

Statistical Errors

$$\sigma = \frac{1}{n} \ln \frac{N_2' N_o}{N_o' N_2}$$

Let $\Delta\sigma$ = standard deviation in σ due to statistical fluctuations.

By the theory of statistical error propagation

$$(\Delta\sigma)^2 = \left(\frac{\partial\sigma}{\partial N_2'}\right)(\Delta N_2)^2 + \left(\frac{\partial\sigma}{\partial N_2}\right)^2 (\Delta N_2')^2$$

$$\therefore \Delta\sigma = \frac{1}{n}\sqrt{\left(\frac{\Delta N_2}{N_2}\right)^2 + \left(\frac{\Delta N_2'}{N_2'}\right)^2}$$

But ΔN_2 = standard deviation in N_2, which is given by the fluctuation in the number of events taking place.

$$\therefore \quad \Delta N_2 = \sqrt{N_o - N_2}$$

Similarly $\Delta N_2' = \sqrt{N_o' - N_2}$

where $\Delta \sigma = \frac{1}{n} \sqrt{\frac{N_o - N_2}{N_2^2} + \frac{N_o' - N_2'}{N_2'^2}}$

and $\frac{\Delta \sigma}{\sigma} = \frac{\sqrt{\frac{N_o - N_2}{N_2^2} + \frac{N_o' - N_2'}{N_2'^2}}}{\ln \frac{N_2' N_o}{N_o' N_2}}$

Sample Energy Calculation

340 Mev = proton beam energy

5 Mev = energy loss in stillbene crystals

$\therefore$ 335 Mev = energy of protons entering attenuator

R (335 Mev) = 91.5 gms/cm^2 copper

attenuator = 28.0 gm/cm^2 copper or equivalent

$\therefore$ Residual Range = 63.5 gms/cm^2 copper

$\therefore$ 268 Mev = proton energy corresponding to range of 63.5 gms/cm^2 copper and is the energy at which protons, suffering no inelastic collision, leave the attenuator

R (268 Mev) = 63.5 gms/cm^2 copper

Absorber = 56.5 gms/cm^2 copper

$\therefore$ Residual Range = 7.0 gms/cm^2 copper

$\therefore$ 75 Mev = energy of protons leaving absorber and entering counter 3

Also 250 Mev = energy corresponding to a range of 56.3 gms/cm^2 of copper, the absorber thickness

$\therefore$ 268 Mev - 250 Mev = 18 Mev = energy that must be lost by the proton in an inelastic collision, if it is to stop in the absorber.

Average Energy of Protons in the Attenuator

Let $\bar{E}$ = average energy in the attenuator

E_1 = entrance energy of proton

R_1 = range corresponding to E_1

E_2 = exit energy of proton

R_2 = range corresponding to E_2

We assume that over the energy intervals considered we can write $E = K R^{\alpha}$ where K and α are constants and α can be evaluated from:

$$\alpha = \frac{d\,(\ln E)}{d\,(\ln R)} = \frac{\ln E_1/E_2}{\ln R_1/R_2}$$

Then $$\bar{E} = \frac{\int_{R_2}^{R_1} E\, d R}{\int_{R_2}^{R_1} d R} = \frac{\int_{R_2}^{R_1} K R^{\alpha}\, d R}{R_1 - R_2}$$

or $$\bar{E} = \frac{K}{\alpha + 1} \frac{R_1^{\alpha+1} - R_2^{\alpha+1}}{R_1 - R_2} = \frac{E_1 R_1 - E_2 R_2}{(\alpha + 1)(R_1 - R_2)}$$

ERRORS

It is difficult to estimate the total experimental errors other than statistical. However, some attempt in this direction seems called for.

By the range method used, the stopping powers of the various attenuators were checked to approximately 1/2 gm of equivalent copper. From the slope of the range curve and the running points chosen, this could introduce an error of about 1 percent in the double to triple coincidence ratio.

The error due to diffraction scattering appears negligible. Using the measured values of $d\sigma/d\theta$ of Richardson[11] for carbon at 340 Mev, the contribution to the cross section by protons scattered more than 20° is found to be less than 2 millibarns. At the lower energies the increase in the solid angle subtended by the rear counter almost compensates for the wider diffraction pattern so that the contribution to the measured cross section because of wide diffraction scattering is less than 3 millibarns. For the elements heavier than carbon and beryllium this effect is completely negligible, since the diffraction pattern becomes quite narrow.

The error due to the spurious counts caused by the production of neutrons in the attenuator and absorber is small. The number of neutrons produced and detected by counter 3 is checked by using slightly more than a range of copper absorber. For the various attenuators and for the internal absorber calibration run, the percentage of triple coincidences due to neutrons is 0.8 percent, 0.3 percent. Only the change in the number of neutron counts causes an error in the measured cross section.

The error due to shifts in the beam level is negligible. Increasing or decreasing the beam by a factor of two changed the measured coincidence ratios by 0.5 percent. It is possible to hold the beam level constant to within 20 percent, thus introducing a maximum error of 0.1 percent.

If we assume no other experimental errors of consequence exist, the total possible systematic error in the true attenuation factor, $f = \frac{N_2 N_o'}{N_o N_2'}$ = the fraction of protons that pass through the attenuator with no inelastic collision, is approximately 1.4 percent. Thus since

$$f = e^{-n\sigma}$$

$$\frac{\Delta\sigma}{\sigma} = \frac{\Delta f}{f \ln f}$$

Therefore:

For $\bar{E} = 305$ Mev $\quad \ln f = 0.16$

Possible systematic error $= \frac{\Delta\sigma}{\sigma} = 9$ percent

For $\bar{E} = 240$ Mev $\quad \ln f = 0.15 \quad \frac{\Delta\sigma}{\sigma} = 10$ percent

For $\bar{E} = 185$ Mev $\quad \ln f = 0.10 \quad \frac{\Delta\sigma}{\sigma} = 14$ percent

These are believed to be the maximum systematic errors possible in the measured cross sections. The final check on the cross sections and assumptions about errors used above will be made when the experiment is done by some independent method.

RESULTS AND CONCLUSIONS

Table I lists the measured cross sections for each of the elements and energy bands considered in the experiment. The errors listed are the standard deviations due to statistics.

Table II lists for comparision the measured absorption and diffraction cross sections for protons and neutrons in the energy region 300-180 Mev. Considering the probable errors in these cross sections, one can conclude that the results do not disagree with the hypothesis that the absorption and diffraction effects for 300 Mev neutrons and protons are essentially the same.

One rather striking effect, however, is the ratio σ_d/σ_a . In the original theory of the transparent nucleus, it was not expected that this ratio would be as small as it appears from the measured cross sections. However, Fernbach[12] in an extension of the theory to higher energies found that he could predict a comparable ratio by assuming a zero shift in wave-length of the incoming nucleon when it entered the nucleus. This is to be expected, since a high energy particle has such a short de Broglie wave-length that it interacts with only the closest nucleons and hence feels no average potential due to all the nucleons in the nucleus.

Thus far the transparent nucleus theory is in reasonable agreement with the experimental data. If one accepts the proton data and calculates the value of K from the ratio $\sigma_a/\pi R^2$ and the curve $\sigma_a/\pi R^2$ vs. KR given in Fig. 7, the values obtained show a consistent variation with respect to A. The value of K changes by a factor of two in going from Be to U for all three energy bands. This might be explained by

assuming that the exclusion principle effect becomes more important with increasing A. This would cause a decrease in the effective nucleon-nucleon cross sections inside the nucleus. However, until the results are duplicated by an independent method such ideas must remain speculative. The neutron data exhibits some change in K with increasing A but nothing comparable to the proton data.

The measured values of σ_a for protons are plotted against energy in Fig. 9. The πR^2 values of the various nuclei are plotted at zero energy. The straight lines down through the points have no real significance, since the cross section is very likely not a simple exponential function of energy. Lacking any other data, however, the lines represent as good extrapolated values of σ_a as are available at present.

In Fig. 10 the cross sections are plotted against A on a log-log scale. The points fall reasonably well on the three parallel straight lines. The slope of the lines is found to be 0.73. This implies that σ_a varies as $A^{2/3} \times A^{1/16}$. The $A^{2/3}$ factor giving the geometrical area of the nucleus and the $A^{1/16}$ the relative opaqueness. Warren Heckrotte predicts, from an analysis of Fernbach's theory, a power law of $A^{0.78}$. The agreement is reasonable in consideration of the 10 percent probable errors in the cross sections.

One hopes that a better method of measuring σ_a for protons will become available, since much interesting information about the nucleus can be extracted from accurate absorption and diffraction cross section data. It would be interesting to repeat the experiment using smaller amounts of absorber behind the attenuator to check whether this method of energy discrimination introduces a systematic error. At the same

time the inelastically forward scattered protons could be studied. Unfortunately, this requires a large amount of running time on the cyclotron.

With the advent of higher proton energies, faster electronics, and a better beam duty factor, the experiment can be performed again, using essentially the same method, to obtain more accurate and more detailed results.

ACKNOWLEDGMENTS

The author wishes to thank Drs. R. L. Thornton, B. J. Moyer, and O. Chamberlain for their help and encouragement at various times. He also wants to thank all the cyclotron operators for their cooperation in running the machine under somewhat trying conditions.

This work was done under the auspices of the Atomic Energy Commission.

Table I

Element	335 - 270 Mev E = 305 Mev $\sigma_a \pm \Delta\sigma_a$ in barns	270 - 205 Mev E = 240 Mev $\sigma_a \pm \Delta\sigma_a$ in barns	205 - 160 Mev E = 185 Mev $\sigma_a \pm \Delta\sigma_a$ in barns
Be	0.151 ± 0.004	0.169 ± 0.006	0.172 ± 0.008
C	0.187 ± 0.006	0.202 ± 0.007	0.204 ± 0.012
Al	0.334 ± 0.009	0.383 ± 0.012	0.408 ± 0.025
Cu	0.608 ± 0.022	0.667 ± 0.031	0.746 ± 0.045
Pb	1.48 ± 0.06	1.57 ± 0.07	1.55 ± 0.11
U	1.60 ± 0.06	1.77 ± 0.07	1.90 ± 0.13

$\Delta\sigma_a$ = standard deviation

Table II

Element	Protons 305 Mev σ_a	πR^2	$\frac{\sigma_a}{\pi R^2}$	10^{12}/cm K	$\sigma_d(13)$	σ_d/σ_a	Neutrons 300 Mev $\sigma_a(8)$	$\sigma_d(8)$	σ_d/σ_a	10^{12}/cm K
Be	0.151	0.256	0.590	2.5						
C	0.187	0.310	0.604	2.4	0.098	0.52	0.203	0.079	0.39	2.7
Al	0.334	0.530	0.630	2.0	0.201	0.60	0.390	0.187	0.48	2.7
Cu	0.608	0.934	0.652	1.6	0.515	0.85	0.755	0.410	0.54	2.6
Pb	1.48	2.07	0.714	1.3	0.934	0.63	1.72	1.34	0.78	1.9
U	1.60	2.27	0.705	1.2						
				240 Mev						
Be	0.169	0.256	0.66	3.0						
C	0.202	0.310	0.65	2.7						
Al	0.383	0.530	0.72	2.6						
Cu	0.667	0.934	0.72	1.9						
Pb	1.57	2.07	0.76	1.5						
U	1.77	2.27	0.78	1.5						

All cross sections are in barns

K values are in units of 10^{12}/cm

Table II
(continued)

Element	Protons 305 Mev σ_a	πR^2	$\frac{\sigma_a}{\pi R^2}$	10^{12}/cm K	$\sigma_d(13)$	σ_d/σ_a	Neutrons 300 Mev $\sigma_a(8)$	$\sigma_d(8)$	σ_d/σ_a	10^{12}/cm K
				185 Mev						
Be	0.172	0.256	0.67	3.2						
C	0.204	0.310	0.66	2.8						
Al	0.408	0.530	0.77	3.0						
Cu	0.746	0.934	0.80	2.5						
Pb	1.55	2.07	0.75	1.5						
U	1.90	2.27	0.84	1.9						

All cross sections are in barns

K values are in units of 10^{12}/cm

REFERENCES

1. R. Sherr, Phys. Rev. 68, 240, (1945)

2. R. H. Hildebrand and C. E. Leith, Phys. Rev. 80, 842, (1950)

3. L. J. Cook, E. M. McMillan, J. M. Peterson, and D. C. Sewell, Phys. Rev. 75, 7, (1949)

4. J. De Juren and B. J. Moyer, Phys. Rev. 81, 919, (1951)

5. R. Fox, C. Leith, L. Wouters, and K. R. MacKenzie, Phys. Rev. 80, 23, (1950)

6. R. Hildebrand, D. Hicks, and W. Harper, U. C. Radiation Laboratory Report UCRL-1305 (a summary of neutron data as of May, 1951)

7. J. De Juren (Thesis), Phys. Rev. 80, 27, (1950)

8. W. Ball (Thesis), U. C. Radiation Laboratory Report UCRL-1938

9. S. Fernbach, R. Serber, and T. Taylor, Phys. Rev. 75, 1352, (1949)

10. C. J. Bakker and E. Segrè, Phys. Rev. 81, 489, (1951)

11. R. Richardson, W. Ball, C. E. Leith, and B. J. Moyer, Phys. Rev. 83, 859, (1951). Phys. Rev. 86, 29, (1952). R. Richardson (Thesis), U. C. Radiation Laboratory Report UCRL-1408

12. S. Fernbach (Thesis), U. C. Radiation Laboratory Report UCRL-1382

LIST OF FIGURES

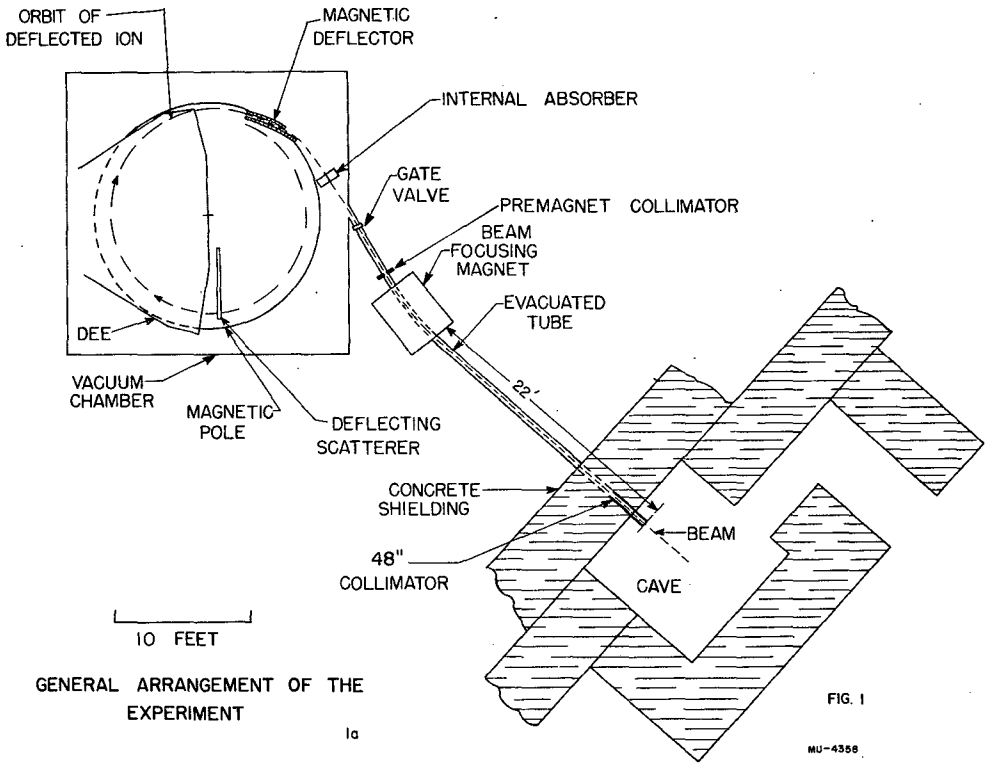

GENERAL ARRANGEMENT OF THE EXPERIMENT

FIG. 1

1a

EQUIPMENT IN THE CONE AND THE
ELECTRONIC CIRCUITS

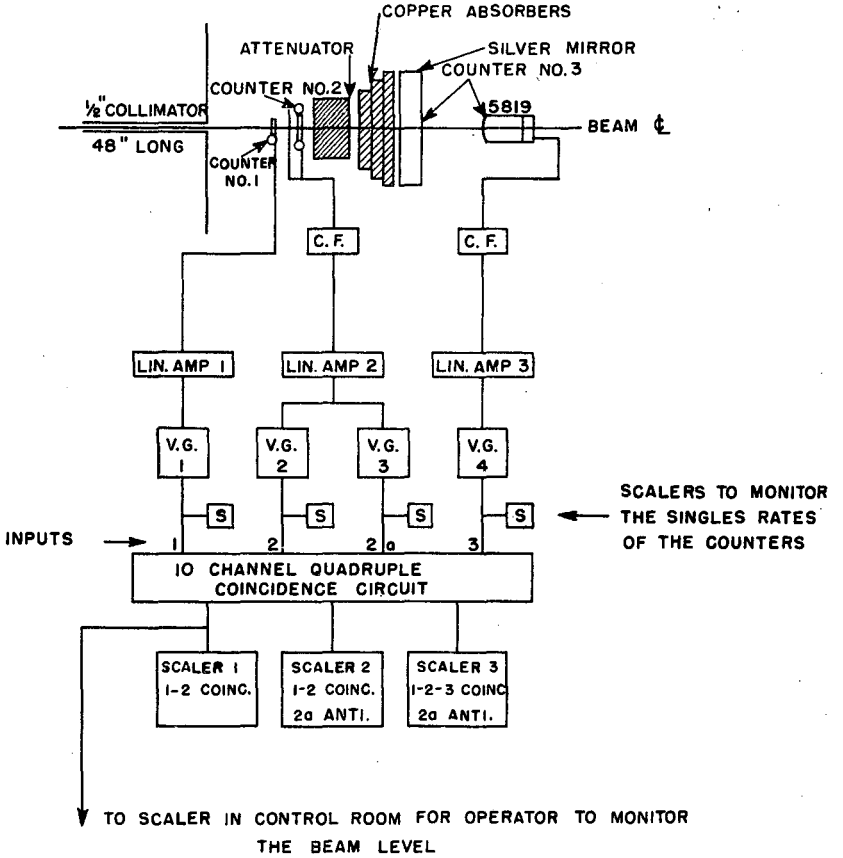

FIG. 2

MU-4359

201461

DETAIL OF THE COUNTERS, ATTENUATOR, AND ABSORBERS

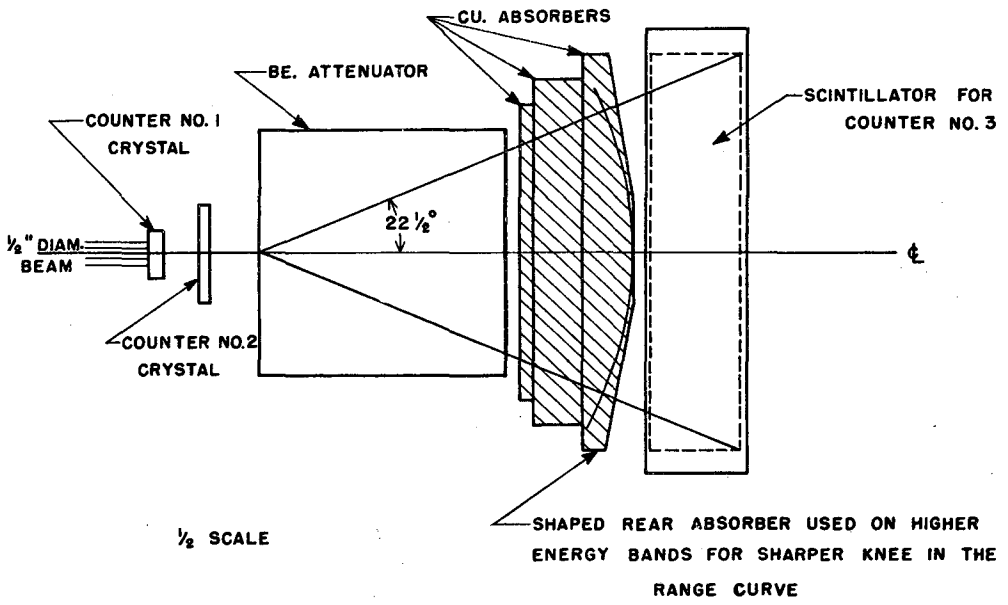

FIG. 3

MU-4360

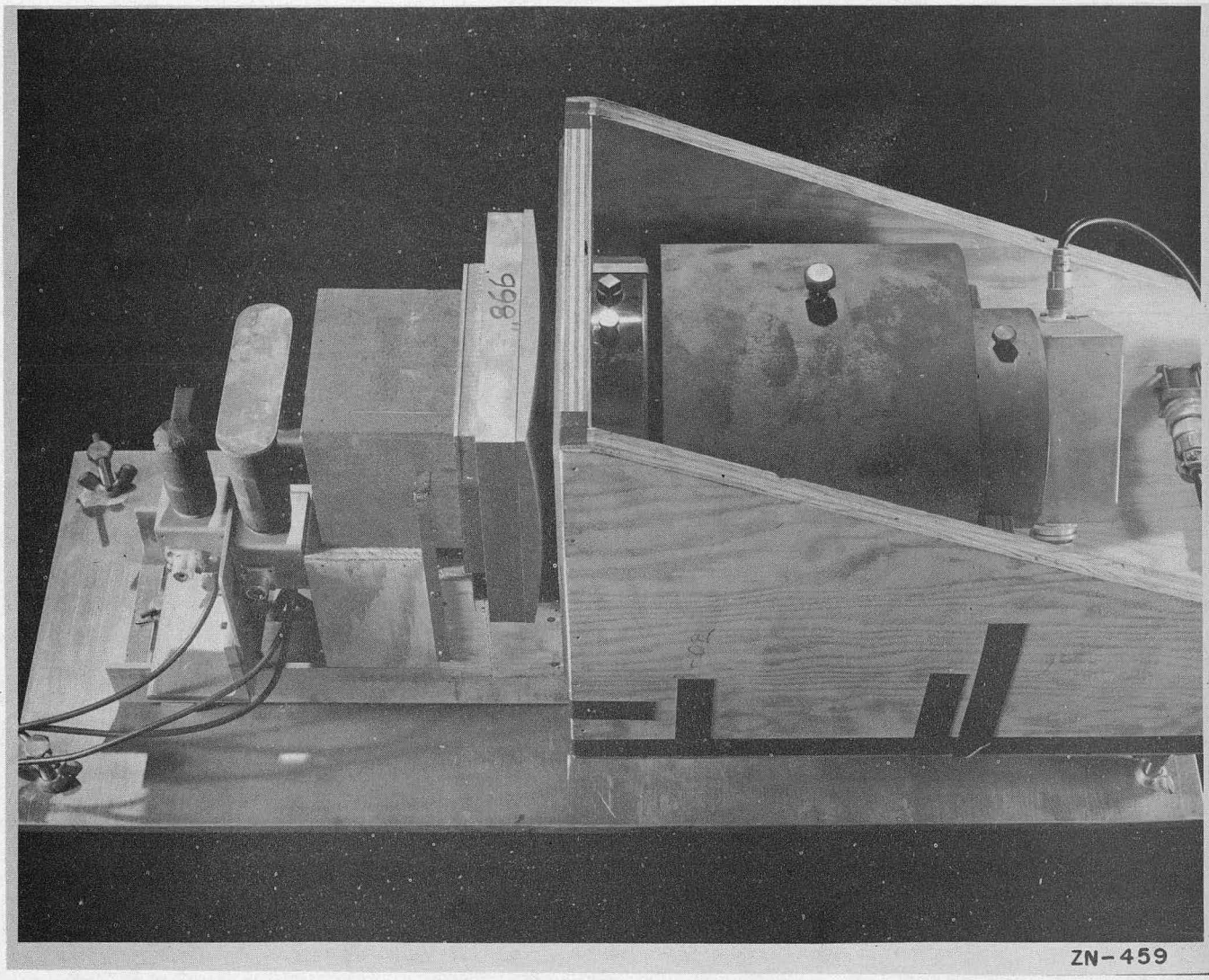

Fig. 4

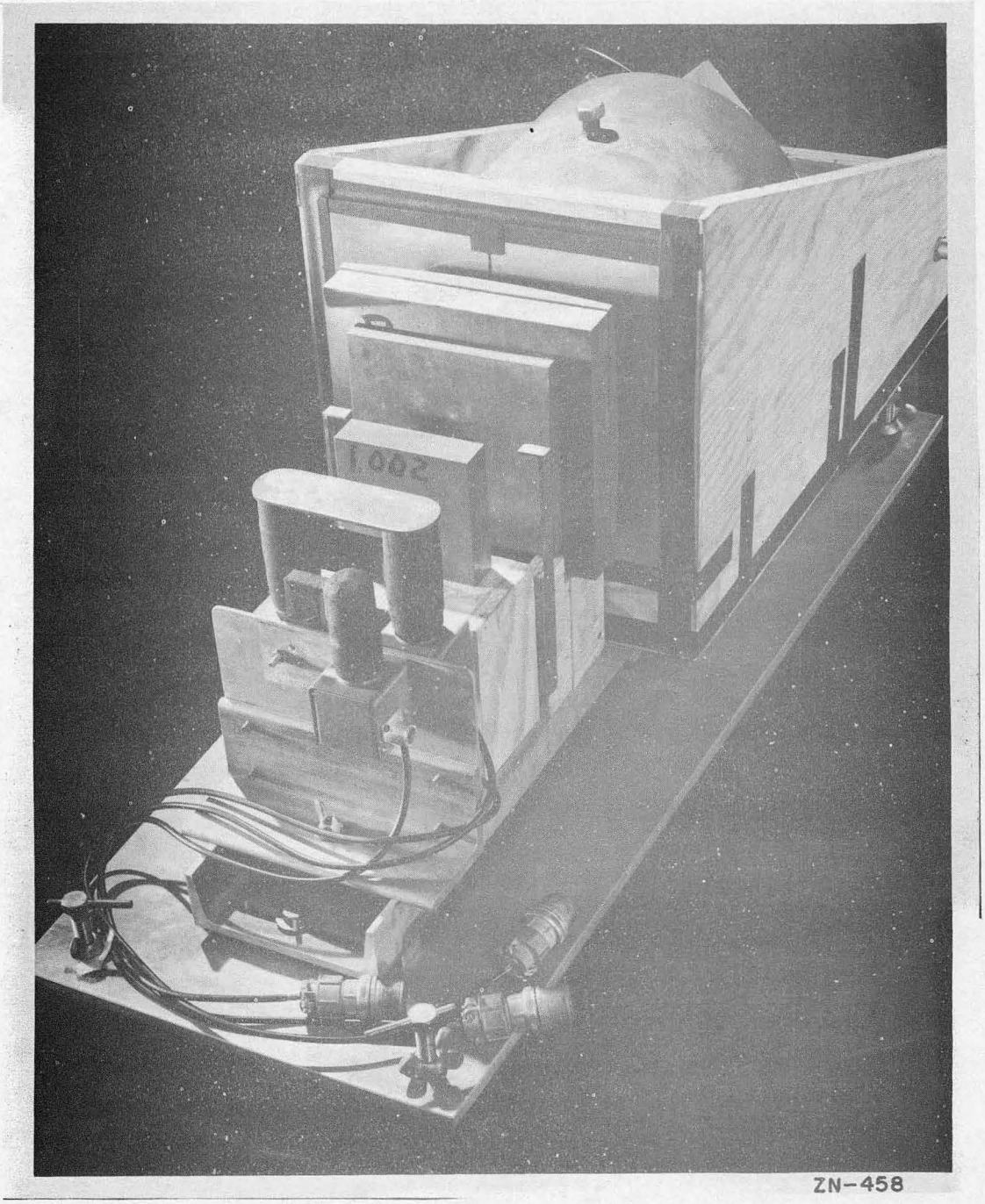

Fig. 5

FIG. 6

DISCRIMINATOR ADJUSTMENT OF THE

PULSE HEIGHT COUNTER

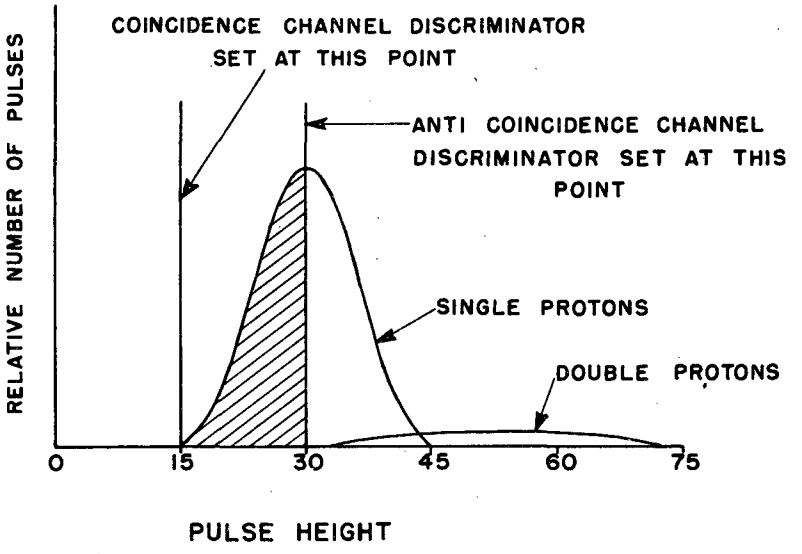

MU-4361

ABSORPTION CROSS SECTION = $\frac{\sigma_a}{\pi R^2}$

vs.

NUCLEAR TRANSPARENCY = KR = R/λ

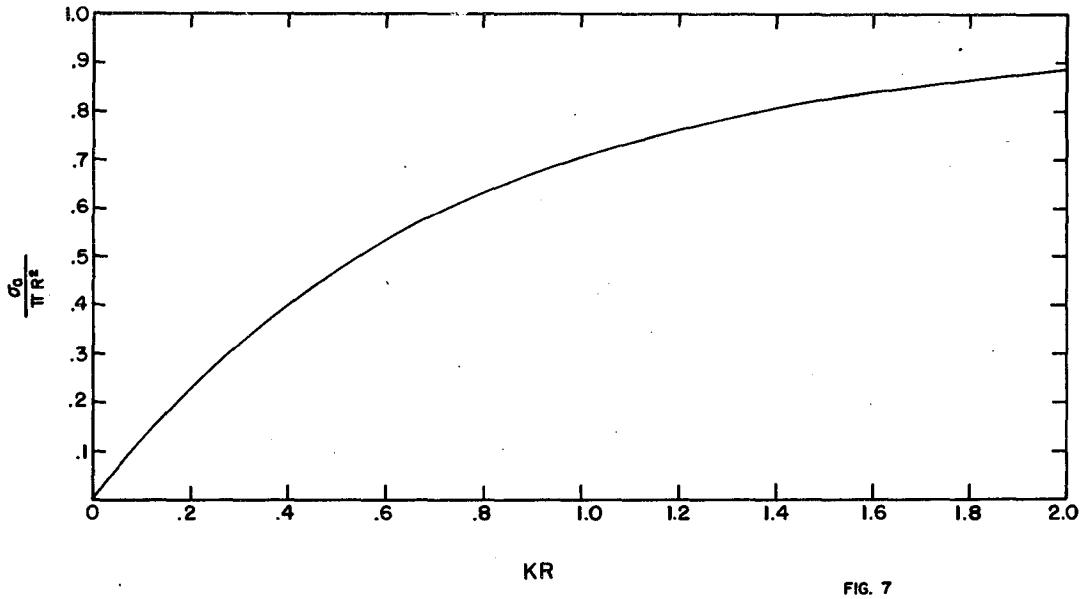

FIG. 7

MU-4362

INTEGRAL RANGE CURVES

FOR COPPER

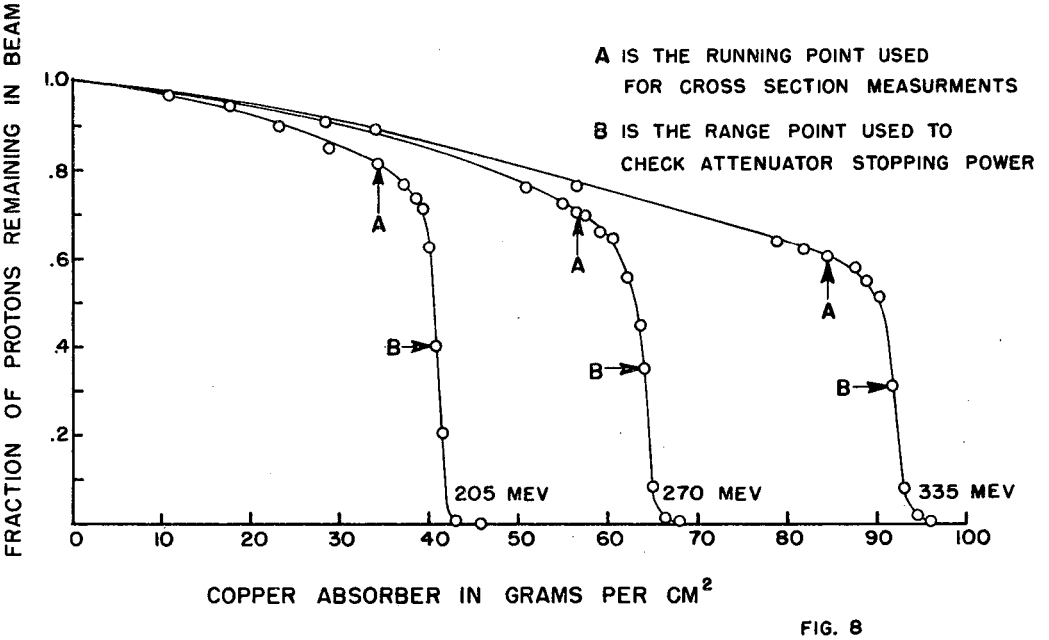

FIG. 8

MU-4363

PROTON ABSORPTION CROSS SECTIONS
VS.
ENERGY

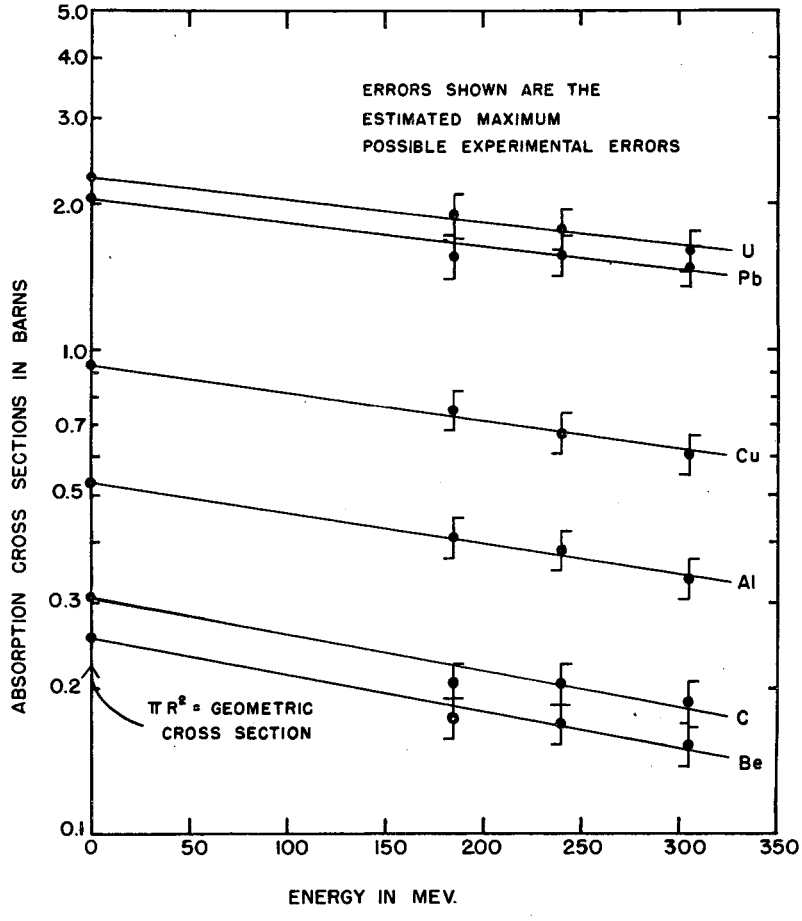

FIG. 9

MU-4364

PROTON ABSORPTION

CROSS SECTIONS VS. ATOMIC NUMBER

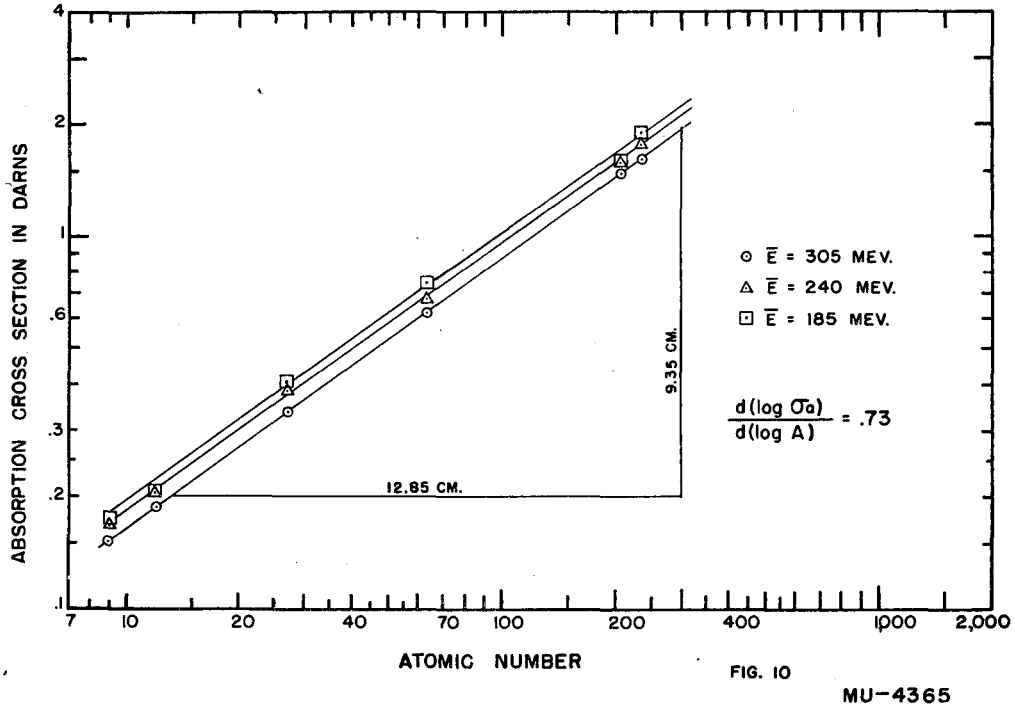

FIG. 10

MU-4365